Safety of Flawed Seamless Gas Cylinders

R. Kieselbach

ABSTRACT

Welded and seamless gas bottles are probably among the most frequently used transportable pressure vessels. The risk involved in the use of these vessels includes their bursting and the explosion of gas leaking from them. To mitigate these risks, regulations both national and international were introduced concerning the design, materials, testing, and approval of gas bottles. Recently recommendations on nondestructive testing by ultrasonics were developed by several national and international authorities. To be able to use ultrasonic testing, it is necessary to define an acceptance level or a critical flaw size. This is only possible if the material properties, that is, strength and toughness, and the stresses are known and if there is a reliable method for assessment available. The results of burst and pulsation tests with artificially flawed seamless high-pressure gas bottles are presented and compared with the results of several risk-assessment methods that were originally developed for nuclear pressure vessels.

At present (1985) in Switzerland the number of gas cylinders that are subject to the regulations on testing and approval (1-3) is estimated at approximately 3 million. Because of the elastic energy of the compressed gas stored in these containers, there exists a substantial risk if the container bursts, particularly if the material exhibits brittle behavior or if combustible gases are set free by leakage. The energy of the compressed gas that is stored, for example, in a typical container of 50 L with a filling pressure of 200 bar is about 0.25 kW·hr and is equivalent to the explosive power of 0.2 kg of trinitrotoluene (TNT). Although leaking can be prevented by careful handling and inspection, the brittle fracture of containers with flaws may occur suddenly and without warning.

In the regulations of most countries for gas cylinders, initially and periodically afterwards, only visual inspection and a hydraulic pressure test are necessary, but in some countries ultrasonic testing as a modern means of nondestructive testing has been incorporated into the regulations (4).

Experience has also shown that it rarely happens that a gas cylinder leaks or bursts during periodic hydraulic testing, even if there are flaws of considerable depth in the wall of the container. This proves that ultrasonic testing should be performed with all gas cylinders for higher pressure (e.g., that for natural gases) because even small defects can be detected; for example, a crack 0.01 mm wide and 0.2 mm deep is still easily found.

In many testing regulations an admissible crack depth of 5 percent of the wall thickness is prescribed (Figure 1) without there being a theoretical or experimental foundation for this value. In this paper a criterion for critical flaw size is investigated.

EXPERIMENTAL INVESTIGATIONS

Test Material

For the experimental studies a number of high-pressure gas cylinders were used that had been sorted out because of flaws in their manufacture. The cylinders were made of a quenched and tempered steel (34CrMo4) and had approximately 50-L capacity, a cylindrical length of approximately 1600 mm, an outer diameter (Da) of approximately 220 mm, and a wall thickness (t) of 6 mm.

The tests for strength and toughness were performed on specimens taken in both the axial and the circumferential directions. The fracture toughness was measured with CT-specimens with a ligament (W) of 20 mm and a thickness of 5.5 to 6 mm that were taken out of the wall of the cylinders. The value of KJIc was determined according to ASTM E813-81 by using that value of the J-integral at which the

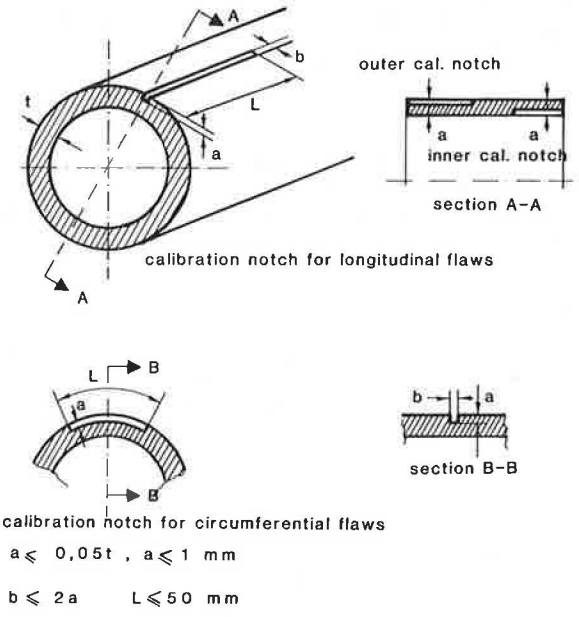

FIGURE 1 Calibration piece for ultrasonic testing of gas cylinders.

first stable crack growth sets in. For comparison the KIc-value according to ASTM E399-81 was also determined and found to be invalid.

Specifications of the Test Materials

The measured values of the mechanical tests are shown in Table 1, in which the Kc-value according to a correlation of Maxey (5) is also shown for comparison. The percentage of each component in the chemical analysis of the steel of the tested cylinders is as follows: carbon, 0.33; silicon, 0.25; manganese, 0.72; phosphorus, 0.013; sulfur, 0.005; chromium, 1.14; molybdenum, 0.16; nickel, 0.35; and copper, 0.26 percent.

TABLE 1 Mechanical Properties of Steel 34CrMo4

	Orientation	
	Longitudinal	Transverse
Rp 0.2 (N/mm^2)	761	1010
Rm (N/mm^2)	1070	1070
A5 (%)	11.2	12.8
Z (%)	24	28.5
Ak, ISO-V, RT (J)	13	52
Ak, ISO-V, −20° C (J)	12	49
KJIc (N/mm$^{3/2}$)	4835 ± 263	3480 ± 196
KIc (N/mm$^{3/2}$)	2649 ± 172	2551 ± 139
Kc (Maxey) (N/mm$^{3/2}$)	5105	10 209

Results of Burst and Pulsation Tests

Practical Performance

The burst and pulsation tests were performed mainly with a servohydraulic transformer with a maximum water pressure of 600 bar. By using the servohydraulic control, arbitrary pressure and time functions could be chosen. A part of the tests was not performed with water but with nitrogen as a pressurizing agent. In these tests a membrane compressor with a final pressure of 1000 bar was used. In the tests with this compressor it was necessary to use a special test range with shelters.

Burst Tests

The burst tests were performed with the notched gas cylinders shown in Figures 2 and 3 with different proportions of gas or liquid content. The results are shown in Table 2.

Pulsation Tests

The aim of the pulsation tests, which were performed with water as pressurizing agent on cylinders notched according to Figure 2 and with the transformer mentioned earlier at a pressure of 20 to 200 bar, was the determination of the final crack depth at which failure occurs. In Tests 38-45 the frequency of pulsation was 1 cycle/min with a rise time of 5 sec and a holding time on pressure of 48 sec. In the other tests a frequency of 4 cycles/min without a holding time was used. The fracture was always accompanied by very slight deformation and large final depth of the fatigue crack (Figures 4 and 5). The results are shown in Table 3.

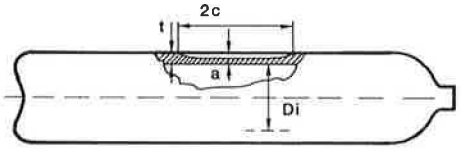

FIGURE 2 Gas container with longitudinal notch.

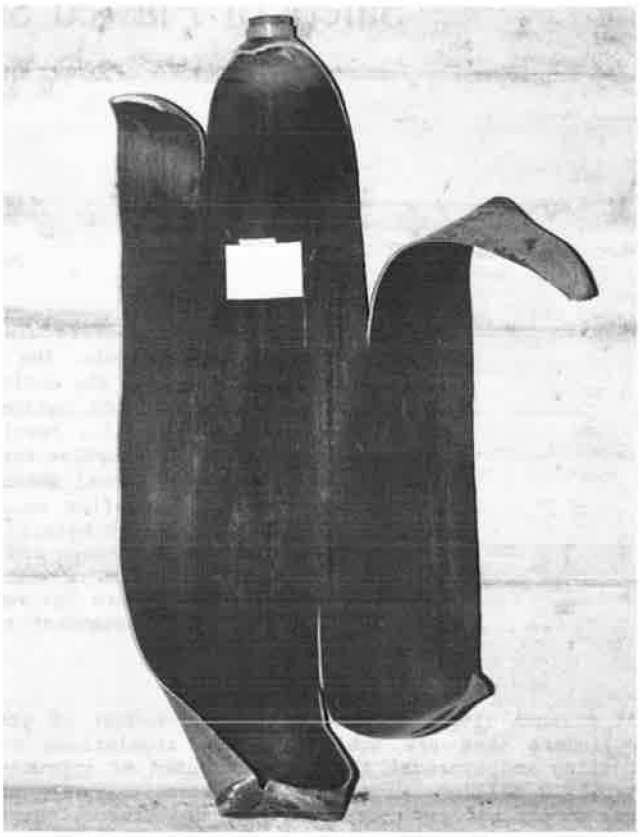

FIGURE 3 Longitudinally notched gas cylinder that burst pneumatically at approximately 230 bar.

TABLE 2 Results of Burst Tests

Test No.	D (mm)	t (mm)	a_0 (mm)	$2c_0$ (mm)	$2c_0'$ (mm)	$2c_e$ (mm)	pBurst (bar)	Gas Content (%)
1	221.1	6.4	3.5	300	333	1150	230.8	~11
2	221.9	6.3	2.5	300	333	1448	299.5	
3	222.1	6.4	3.5	150	183	896	207.8	
4	222	6.2	3	150	180	896	216.1	
5	222	6.2	2.5	150	178	850	309.6	
6	221.6	6	2	150	175	1484	364.3	
7	221.8	6	2.5	150	178	1220	297.6	~51
8	221.8	6.1	2.6	150	178	1468	343.7	
9	221.8	5.8	2.8	150	179	1280	275.9	
10	223.1	6.1	3	150	180	1086	265.8	
11	222.7	6.2	3.1	150	181	1280	271.7	
12	222.5	6	3.3	150	182	924	203	
13	221	6	3.4	150	182	968	198	
15	221	6	2.3	150	177	6266	310.4	100
16	221	6.4	2.5	150	178	6255	317.7	
17	221	6	2.8	150	179	6835	292.1	
18	221	6.2	3	150	180	6205	312.9	
19	221	6	3.3	150	182	6565	193.7	
20	221	6.1	3.5	150	183	6550	227.9	
21	221	6	2	300	325	5615	374.6	
22	221	5.9	3.5	300	333	5445	144.8	

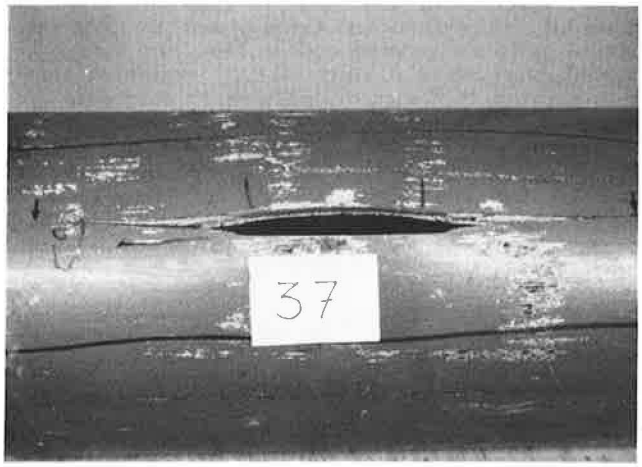

FIGURE 4 Notched gas cylinder after breakthrough of the crack.

FIGURE 5 Fracture surface of notched gas cylinder after pulsation with 200 bar (from top: notch, fatigue crack, final fracture).

TABLE 3 Results of Pulsation Tests

Test No.	No. of Cycles	a_0 (mm)	a_e (mm)	$2c_0'$ (mm)	$2c_e$ (mm)	t (mm)	pBurst (bar)
23	5,439	2	5.4	50	50	5.80	200
24	4,257	2	5.6	50	50	5.90	200
25	5,346	2	5.5	50	50	5.90	180.7
26	7,065	2	5.5	50	50	6.00	200
27	7,631	2	5.7	50	50	6.2	193
28	1,281	2	5.5	75	76.8	6.00	191.7
29	1,513	2	5.3	75	75	5.8	196
30	5,674	2	5.4	75	75	6.20	200
31	1,730	2	5.2	75	75	5.8	200
32	4,470	2	5.1	75	75	6.00	200
33	8,239	2	5.6	125	370	6.1	195.3
34	1,120	2	5.2	125	430	5.9	193.3
35	1,854	2	5.2	125	570	6.1	200
36	716	2	4.9	125	470	5.8	200
37	1,369	2	5.3	125	360	5.9	200
14	5,434	2	5.3	150	470	5.90	200
38	21,137	1	5.8	50	68	—	200
39	10,800	1	5.9	50	68	6.1	200
40	8,950	1	5.9	50	68	6.1	200
41	2,699	2	5.4	50	75	6.0	200
42	5,143	2	5.1	50	75	5.7	200
43	3,307	2	5.6	50	75	6.1	200
44	4,612	2	5.4	50	75	5.9	200
45	1,275	2	5.6	50	75	6.2	200

Note: Depth of notch 1 mm, 13,630 ± 6,570 cycles. Depth of notch 2 mm, 3,820 ± 2,340 cycles.

ASSESSMENT OF FRACTURE BEHAVIOR

Stress in Cylinder Containing Axial Surface Flaw

The circumferential stress at fracture may be estimated as

$$ST,fracture = RM(t - a)/t \quad (1)$$

The approximation of Equation 1 gives the values shown in Table 4. A more exact formula for the burst pressure was found by Folias (6):

$$pBurst = \{25/D \cdot Sf[t/(a - 1)]\}/\{[t/(a - 1)]/M\} \quad (2)$$

$$M = [1 + 1.61 \cdot (2c^2/Dt)]^{1/2} \quad (3)$$

Here the flow stress is

$$Sf = (Rp0.2 + Rm)/2.4 \quad (4)$$

TABLE 4 Burst Pressure of Containers with Surface Flaw and with Semielliptical Surface Crack

Container with Surface Flaw		Container with Surface Crack		
a (mm)	p (bar)	2c (mm)	a (mm)	p (bar)
1	486	50	1	465
2	389	100	1	444
3	292	50	2	421
4	195	100	2	380
		50	3	364
		100	3	307
		50	4	286
		100	4	222

and the factor 2.4 may also take values between 1.97 and 2.72 corresponding to the strength of the material used.

The final pressures that were actually found in the experiments are shown in Figure 6 in relation to the ratio of crack depth to wall thickness and compared with these methods of assessment.

The critical pressure for a cylinder with a semielliptical surface crack is given by Equation 2 (Table 4).

Assessment According to Kiefner/Battelle

For the failure of pipelines, a semiempirical formula was proposed by Kiefner that combines the geometry of the flaw and the material properties flow stress and toughness (5). This formula is supposed

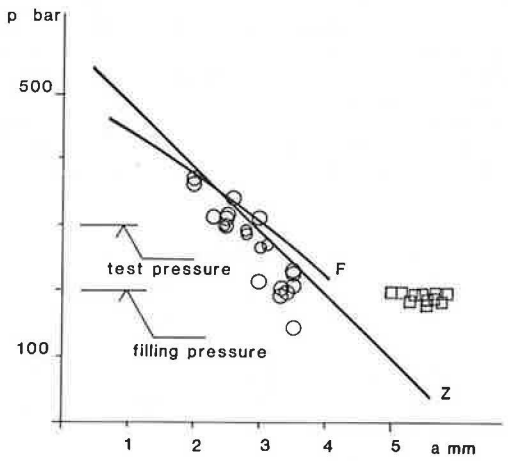

FIGURE 6 Comparison of the pressure for failure due to plastic collapse with test results [Z, Equation 1; F, after Folias (6); 2c = 100 mm; circles = burst tests; squares = pulsation tests].

to judge whether failure may occur under the given conditions and what kind of failure, ductile or brittle.

$$(Kc/Sf)^2 = 8c/\pi \ln[\sec(\pi/2 \cdot MP \cdot St/Sf)] \quad (5)$$

$$MP = \{[t/(a-1)]/MT\}/[t/(a-1)] \quad (6)$$

$$MT = 1 + 1.255 \cdot 2c^2/Dt - 0.013(2c^2/Dt)^2]^{1/2} \quad (7)$$

This formula actually describes a limiting curve (Figure 7) and the assessment of failure is given by the position of the point determined by the parameters

$$X = (Kc/Sf)^2\pi/(8c)$$
$$Y = St/Sf \cdot MP \quad (8)$$

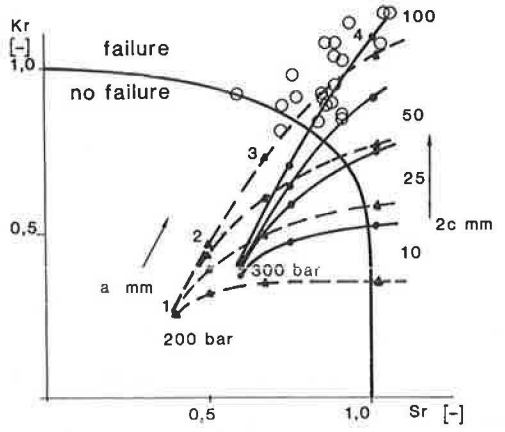

FIGURE 7 Comparison of test results with the assessment according to R6/EPRI (circles = burst tests).

If the parameter X is greater than 3, failure will be by plastic collapse; if X is less than 0.5, failure will be by brittle fracture.

The magnification of stresses because of the bulging of the cylinder at the tip of the crack is given by the Folias factor (MT) for the crack that has broken through and by MP for the surface crack. Equation 6 is slightly different from Equation 2 because it was found that values calculated from the latter were too conservative. With K = 5105 N/mm$^{3/2}$, one obtains the results of Table 5. Failure by plastic collapse may be excluded because the values of X are always less than 0.5.

The critical crack-size parameters are determined from Figure 8 and the values in Table 6 are derived. If an existing surface crack grows faster in the radial direction of the cylinder than in the axial direction, it will break through and the pressure will be released because of the leak. In this case the cylinder cannot disintegrate by excessive axial crack growth. This sort of behavior is desirable and is judged by the leak-before-break criterion. If in consequence the critical pressure for a surface crack is lower than that for a through crack, leakage will occur first.

For the method of Kiefner/Battelle the limit is reached for those crack-size parameters for which the following holds:

$$MT = MP \quad (9)$$

It this relation is evaluated, one obtains the diagram in Figure 9. Here the failure limits for 200 and 300 bar are indicated and the leak-before-break line divides the field of crack-size parameters into those for leaks and those for breaks.

From Figure 9 it can be determined that at a pressure of 200 bar and a crack length 2c of 54 mm, a leak will occur before a break for cracks deeper than 56 percent of the wall thickness and at 300 bar and a crack length of 33 mm it will occur at more than 51 percent relative crack depth. The points for the parameters of the experiments are all well above the limiting curve (see Figure 8) and far into the linear-elastic region, farther than would have been expected from the previous calculations. This fact indicates that the material has in reality shown a more brittle behavior than would have been expected by the test results of the mechanical properties.

TABLE 5 Assessment According to Kiefner/Battelle *(5)*

2c (mm)	a (mm)	X	Y(limit)	p(limit) (bar)	Y(200 bar)	Y(300 bar)
50	1	0.489	0.580	287	0.404	0.606
100	1	0.245	0.427	202	0.423	0.635
50	2	0.489	0.580	262	0.442	0.663
100	2	0.245	0.427	175	0.490	0.735
50	3	0.489	0.580	230	0.505	0.758
100	3	0.245	0.427	142	0.601	0.902
50	4	0.489	0.580	184	0.631	0.947
100	4	0.245	0.427	104	0.822	1.232
50	6	0.489	0.580	204	0.568	0.851
100	6	0.245	0.427	94	0.913	1.37

Assessment According to R6 or Bloom and Malik (7)

Application of Limiting Curve

In Great Britain the so-called two-parameter approach was developed by the Central Electricity Generating Board (CEGB). This approach uses a relation that has formally the same structure as that of the Battelle formula but is nondimensional with respect to the stress intensity and pressure:

$$Kr = Sr\{8/\pi^2 \ln[\sec(\pi/2Sr)]\}^{-0.5}$$
$$Kr = K1/KIc$$
$$Sr = p/pc \quad (10)$$

$$pc = \{[Sf\ 4t/(D/3)][(1-a)/t]\}/[(1+2a)/D] \quad (11)$$

According to the relations of linear-elastic fracture mechanics, K1 is given by (7,8)

$$K1 = pD/(2t)(\pi a/QF)^{1/2} \quad (12)$$

$$Q = 1 + 4.593(a/2c)^{1.65} \quad (13)$$

$$F = 0.97[M1 + M2(a/t)^2 + M3(a/t)^4] \cdot fc \quad (14)$$

$$M1 = 1.13 - 0.18a/2c \quad (15)$$

$$M2 = -0.54 + 0445/(0.1 + a/2c) \quad (16)$$

$$M3 = 0.5 - 1/(0.65 + a/c) + 14(1 - a/c)^{24} \quad (17)$$

$$fc = 1.152 - 0.05(a/t)^{1/2} \quad (18)$$

Again the safe region is separated from the unsafe region by a limiting curve (see Figure 7). With this approach it can be seen that on one axis the point 0/1 marks the complete brittle fracture and on the other axis the point 1/0 marks fracture by complete plastic collapse and that the real cases may be expected to lie in between.

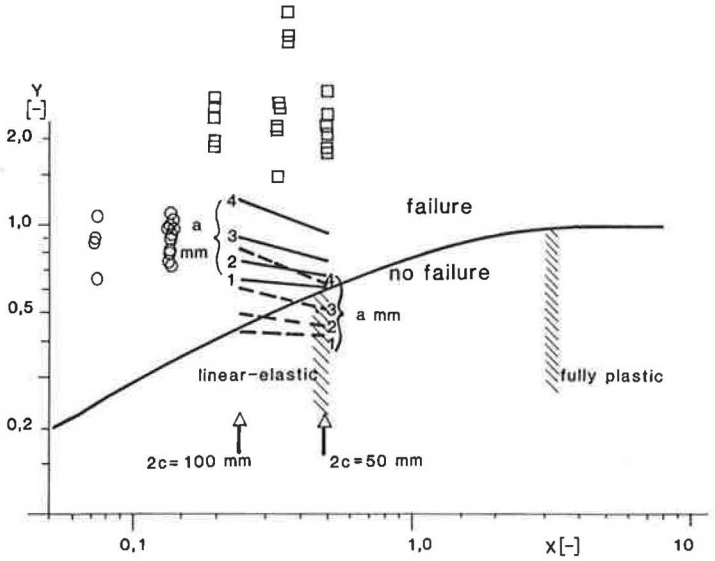

FIGURE 8 Failure curve according to Kiefner/Battelle (*5*) with assessment for different crack depths (a) and lengths (2c) and for internal pressure of 300 bar (solid lines) and 200 bar (dashed lines) compared with test results (circles = burst tests; squares = pulsation tests).

TABLE 6 Critical Crack-Size Parameters According to Kiefner/Battelle (*5*)

2c (mm)	a_c (mm)	p (bar)	a_c/t
50	3.65	200	0.608
50	0.75	300	0.125
100	1.05	200	0.175
100	–	300	–

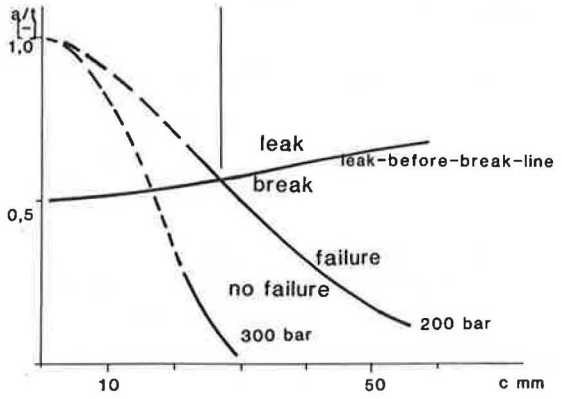

FIGURE 9 Use of leak-before-break diagram derived from the results of Kiefner/Battelle (*5*).

The R6-routine approach was further developed in the United States by the Electric Power Research Institute (EPRI) by allowing a certain amount of pre-critical crack growth. With this development a slight shift of the limiting curve toward higher values of the parameters is achieved. In Equations 10 the stress intensity calculated according to the formulas of Newman-Raju is used. For the assessment one obtains the values in Table 7. It may be clearly seen that the influence of the crack length on the critical crack depth is rather limited.

In Figure 7 the values for 200 and 300 bar are plotted from which it is possible to determine the critical values at the limiting curve, shown in Table 8. The points experimentally found for the pulsation tests are so far away from the limiting curve that it was not possible to plot them on the same scale as that in Figure 7.

TABLE 7 Assessment According to R6/EPRI

a (mm)	p (bar)	Sr	Kr by Crack Length 10 mm	25 mm	50 mm	100 mm
1	200	0.398	0.242	0.26	0.266	0.27
2	200	0.502	0.317	0.391	0.432	0.466
3	200	0.675	0.348	0.5	0.605	0.73
4	200	1.022	0.351	0.580	0.765	1.045
5	200	2.063	0.337	0.624	0.887	1.357
1	300	0.596	0.363	0.389	0.399	0.405
2	300	0.752	0.475	0.586	0.647	0.699
3	300	1.013	0.522	0.749	0.907	1.095
4	300	1.533	0.526	0.870	1.147	1.567
5	300	3.095	0.506	0.936	1.331	2.036

TABLE 8 Critical Values at the Limiting Curve According to R6/EPRI

p (bar)	2c (mm)	a_c (mm)	a_c/t
200	10	3.95	0.657
200	25	3.9	0.65
200	50	3.7	0.62
200	100	3.3	0.55
300	10	2.92	0.487
300	25	2.7	0.45
300	50	2.5	0.42
300	100	2.3	0.38

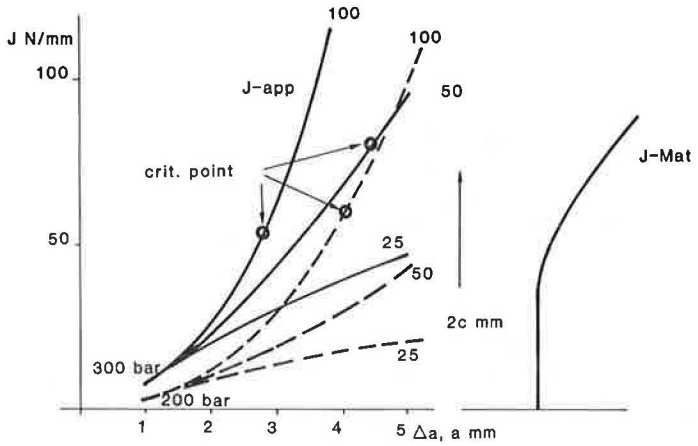

FIGURE 10 Curves for J versus Δa for semielliptical surface crack (7).

TABLE 9 J-Integral for Semielliptical Surface Crack (7)

a (mm)	p (bar)	J (N/mm) by Crack Length 10 mm	25 mm	50 mm	100 mm
1	200	3 133	3 616	3 785	3 900
2	200	5 376	8 179	9 984	11 617
3	200	6 479	13 374	19 581	28 509
4	200	6 591	17 997	31 308	58 420
5	200	6 076	20 831	42 090	98 513
1	300	7 049	8 095	8 517	8 775
2	300	12 070	18 371	22 394	26 139
3	300	14 577	30 012	44 010	64 145
4	300	14 801	40 492	70 382	131 362
5	300	13 697	46 869	94 774	221 763

TABLE 10 Critical Values for Semielliptical Surface Crack (7)

p (bar)	a_o (mm)	a_c (mm)	Δa (mm)	2c (mm)	a_c/t
200	3.6	4.05	0.45	100	0.675
300	2.5	2.8	0.3	100	0.467
300	3.25	4.45	1.2	50	0.742

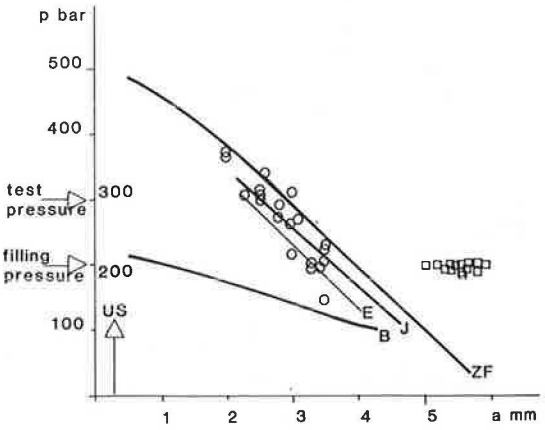

FIGURE 11 Comparison of the different failure criteria with test results [B = Kiefner/Battelle (5), E = R6/EPRI, J = curve of J versus Δa, ZF = superposition of curves Z and F of Figure 9 (circles = burst tests; squares = pulsation tests)].

Elastic-Plastic Fracture Mechanics: Crack Resistance Curve

If the crack resistance curve of the material used and the J-applied curve are known, it is possible to determine the critical crack size, the critical pressure, and the amount of stable crack growth from them. In NP-1931 of EPRI (8), solutions for that purpose are given.

In the tangent point of the curves J(mat) and J(app) the following holds:

$$J(\text{mat}) = J(\text{app})$$
$$\partial J/\partial a|_{\text{mat}} = \partial J/\partial a|_{\text{app}} \qquad (19)$$

From the critical value of J(app) one gets the critical load, hence the critical pressure and the critical crack depth. J(app) for the semielliptical surface crack may be calculated by using the equations of EPRI NP-2431 (7). The corresponding values are shown in Table 9.

Figure 10 again gives the critical values in the tangent points of J(app) and J(mat), which are included in Table 10. Figure 11 shows a comparison of the test results with this assessment.

DISCUSSION OF RESULTS OF BURST AND PULSATION TESTS

If the pressures that were found experimentally are compared in relation to crack depth, it is obvious that the results of the pulsation tests form a separate group: in the pulsation tests a much deeper

TABLE 11 Summary of Critical Crack Size by Assessment and by Experiment

Method	a_c (mm) by Pressure 200 Bar	300 Bar
Plastic flow (Table 4)	3.8	2.8
Semielliptical (Table 4)	4.5	3.2
Kiefner (Table 6)	1.05	–
R6/EPRI (Table 8)	3.3	2.3
J-integral (Table 10)	3.6	2.5
Experimental lower bound	3.25	2.25

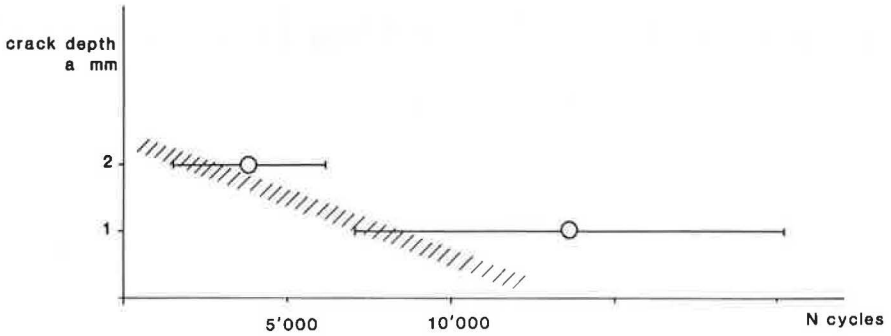

FIGURE 12 Cycles to failure for containers with different initial crack lengths.

crack was necessary for fracture than that in the burst tests. Considering the leak-before-break diagram (Figure 9) one sees that even very deep cracks do not lead to failure if they do not reach a certain length. So it seems that at least in some of the pulsation tests the leak-before-break criterion was met.

If the pressure is increased in a burst test, the flow stress is eventually reached in the remaining part of the wall under the crack (ligament). On the other hand, the pulsation test is performed at a constant pressure amplitude well below the flow stress of the material, so that elastic behavior is observed until fracture occurs, but only in the immediate vicinity of the crack tip. This may also be seen by the fact that the crack does not propagate axially at fracture and that the container does not show any signs of significant plastic deformation in the region of the crack (see Figure 5).

CONCLUSION: ESTABLISHMENT OF CRITERION FOR ELIMINATION OF FLAWED GAS CYLINDERS IN ULTRASONIC TESTING

From the comparison of the results of the different methods of failure assessment it can be seen that an assessment of fracture of a container with a flaw that takes into account only the strength of the material is not sufficient, and only if the toughness is also incorporated into the assessment is a reliable assessment of fracture safety possible.

From the summary of Figure 11 it is to be seen that in the burst tests the critical crack depth at the test pressure was approximately 2.25 mm and at filling pressure approximately 3.25 mm. Table 11 shows that the critical values given by the assessment according to R6/EPRI are the best approximation of the experimental results.

If one postulates for the acceptance level that during the pressure test no failure must occur (which is important for periodic testing), the admissible crack depth with a factor of safety of 2.0 is still approximately 1.1 mm, corresponding to approximately 20 percent of the wall thickness. It would hence be possible to increase the admissible crack depth from 5 to 20 percent of the wall thickness and still have a safety factor of 2.7 for fracture at the filling pressure.

If the admissible crack depth is left at the present value of 5 percent of the wall thickness, the safety factor at test pressure is 7.5 and that at filling pressure is 10.8.

From the pulsation tests it can be seen that a fatigue crack emanating from a notch of 1-mm depth (i.e., 17 percent of wall thickness) needs at least 7,000 cycles at filling pressure to break through; starting with a 2-mm notch depth 1,500 cycles were necessary for leakage (see Figure 12).

When the interval of inspection is 10 years, these 1,500 cycles correspond to 150 cycles of filling per year; hence the cylinder would have to be filled and emptied far more frequently than is to be expected with approximately 250 working days per year. If the admissible crack depth was set at 1.2 mm, the number of cycles until leakage would be at least 5,600; maintaining the 5 percent limit would even yield more than 10,000 cycles to failure.

REFERENCES

1. Verordnung ueber die Pruefung von Druckgefaessen fuer die Befoerderung von Gasen. Swiss Government Regulation 742.441. Bern, Switzerland, 1975.
2. European Agreement Concerning the International Carriage of Dangerous Goods by Road. Economic Commission for Europe/Trans/60 (Vols. 1-3).
3. Ordnung fuer die internationale Eisenbahnbefoerderung gefaehrlicher Gueter [Reglement International Concernant le Transport des Marchandises Dangereuses (RID)]. Office Central des Transports Internationaux par Chemins de Fer (OCTI), Bern, Switzerland, 1985.
4. Specification for Transportable Gas Containers. BS 5045, Part 1. British Standards Institution, London, 1976.
5. B.W. Christ et al. Fracture Analysis of a Pneumatically Burst Seamless-Steel Compressed Gas Container. Special Technical Publication 677. ASTM, Philadelphia, Pa., 1979, pp. 734-745.
6. D. Munz, ed. Leck-vorBruch-Verhalten druckbeaufschlagter Komponenten. VDI-Fortschrittsbericht, Reihe 18, No. 14. VDI-Verlag, Duesseldorf, West Germany, 1984.
7. J.M. Bloom and S.N. Malik. Procedure for the Assessment of the Integrity of Nuclear-Pressure Vessels and Piping Containing Defects. NP-2431, Research Project 1237-2. Electric Power Research Institute, Palo Alto, Calif., 1982.
8. V. Kumar et al. An Engineering Approach for Elastic-Plastic Fracture Analysis. NP-1931, Research Project 1237-1. Electric Power Research Institute, Palo Alto, Calif., 1981.